NIH Public Access
Author Manuscript
Immunity. Author manuscript; available in PMC 2015 September 18.

Published in final edited form as:
Immunity. 2014 September 18; 41(3): 389–401. doi:10.1016/j.immuni.2014.08.015.

The stress-response sensor Chop regulates the function and accumulation of myeloid-derived suppressor cells in tumors

Paul T. Thevenot[1], **Rosa A. Sierra**[1], **Patrick L. Raber**[1,2], **Amir A. Al-Khami**[1], **Jimena Trillo-Tinoco**[1], **Parisa Zarreii**[1], **Augusto C. Ochoa**[1,3], **Yan Cui**[1,2], **Luis Del Valle**[1], and **Paulo C. Rodriguez**[1,2]

[1]Stanley S. Scott Cancer Center. Louisiana State University Health Sciences Center, New Orleans, LA, 70112, USA

[2]Department of Microbiology, Immunology, and Parasitology. Louisiana State University Health Sciences Center, New Orleans, LA, 70112, USA

[3]Department of Pediatrics. Louisiana State University Health Sciences Center, New Orleans, LA, 70112, USA

Summary

Adaptation of malignant cells to the hostile milieu present in tumors is an important determinant for their survival and growth. However, the interaction between tumor-linked stress and anti-tumor immunity remains poorly characterized. Here, we show the critical role of the cellular stress sensor C/EBP-homologous protein (Chop) in the accumulation and immune inhibitory activity of tumor-infiltrating myeloid-derived suppressor cells (MDSCs). MDSCs lacking Chop had decreased immune regulatory functions and showed the ability to prime T cell function and induce anti-tumor responses. Chop expression in MDSCs was induced by tumor-linked reactive oxygen and nitrogen species and regulated by the activating-transcription factor-4. Chop-deficient MDSCs displayed reduced signaling through CCAAT/enhancer-binding protein-β, leading to a decreased production of interleukin-6 (IL-6) and low expression phospho-STAT3. IL-6 over-expression restored immune suppressive activity of Chop-deficient MDSCs. These findings suggest the role of Chop in tumor-induced tolerance and the therapeutic potential of targeting Chop in MDSCs for cancer immunotherapy.

Keywords

MDSCs; C/EBPβ; Chop; integrated stress responses; Interleukin-6; Reactive oxygen species (ROS); peroxynitrite (PNT)

© 2014 Elsevier Inc. All rights reserved.

Correspondence should be addressed to: Paulo C. Rodriguez, PhD. Stanley S. Scott Cancer Center, Louisiana Cancer Research Consortium (LCRC), Louisiana State University Health Sciences Center (LSU-HSC). 1700 Tulane Ave Room 910, New Orleans, LA, 70112, USA, Tel: (504) 210-3324; prodri1@lsuhsc.edu.

Publisher's Disclaimer: This is a PDF file of an unedited manuscript that has been accepted for publication. As a service to our customers we are providing this early version of the manuscript. The manuscript will undergo copyediting, typesetting, and review of the resulting proof before it is published in its final citable form. Please note that during the production process errors may be discovered which could affect the content, and all legal disclaimers that apply to the journal pertain.

Detailed description of Methods and Reagents has been included in the Supplementary Methods section.

NIH-PA Author Manuscript
NIH-PA Author Manuscript
NIH-PA Author Manuscript

NIH-PA Author Manuscript

NIH-PA Author Manuscript

NIH-PA Author Manuscript

Introduction

Inflammatory mediators present in most individuals with cancer inhibit anti-tumor immunity and represent a major limitation in the development of different forms of immunotherapy (Coussens et al., 2013). A characteristic of cancer-linked inflammation is the accumulation of various immune inhibitory populations, including myeloid-derived suppressor cells (MDSCs), regulatory T (Treg) cells, and plasmacytoid dendritic cells (pDCs) (Chen and Mellman, 2013). MDSCs represent a heterogeneous group of myeloid precursors that impair the function of T, NK, and DCs through several pathways including the expression of arginase I, inducible nitric oxide synthase (iNOS), and $Gp91^{phox}$; and the release of reactive oxygen species (ROS), and peroxynitrite (PNT) (Raber et al., 2012). In addition to their immunoregulatory activity, MDSCs also promote tumor angiogenesis and metastasis (Gabrilovich et al., 2012). Two distinct subsets of MDSCs have been identified in mice, granulocytic MDSCs (G-MDSCs, $CD11b^{+}$ $Ly6G^{+}$ $Ly6C^{Int}$) and monocytic MDSCs (M-MDSCs, $CD11b^{+}$ $Ly6G^{lo}$ $Ly6C^{hi}$), both characterized by the expression of $CD11b^{+}$ $Gr1^{+}$ (Movahedi et al., 2008). Although the inhibitory role of MDSCs in anti-tumor immunity is well understood, the central mechanisms governing MDSCs function remain poorly characterized, which has limited the development of strategies to globally block MDSCs activity.

Transcription factors CCAAT/enhancer binding protein β (C/EBPβ) and phosphorylated signal transducer of activator of transcription 3 (phospho-STAT3) centrally regulate MDSCs function and expansion (Corzo et al., 2009; Marigo et al., 2010; Sonda et al., 2013). Three isoforms of C/EBPβ are generated from a single mRNA through alternative protein synthesis (Descombes and Schibler, 1991). C/EBPβ isoforms liver-enriched activator proteins (LAP* and LAP) function as transcriptional activators of chronic inflammation-linked genes, such as interleukin-6 (IL-6) and arginase I (Marigo et al., 2010). Conversely, C/EBPβ liver-enriched inhibitory protein (LIP) lacks DNA transactivation domains and reduces inflammation by blocking C/EBPβ LAP and LAP* signaling (Hattori et al., 2003). MDSCs activity also depends upon phospho-STAT3, which directly induces the expression of arginase I, and $Gp91^{phox}$, and the production of ROS (Vasquez-Dunddel et al., 2013). Although the independent role of C/EBPβ and phospho-STAT3 in MDSCs has been studied, the physiological mediators regulating C/EBPβ and phospho-STAT3 levels in tumor-infiltrating MDSCs remain poorly described.

Metabolic activities in the tumor microenvironment lead to the generation of a hostile milieu characterized by reduced oxygen supply; limited availability of the amino acids arginine, cysteine, and tryptophan; elevated production of ROS and PNT; low pH; defects in glycoprotein and lipid biosynthesis; and glucose starvation linked to tumor glycolysis (Pearce et al., 2013). These mediators of tumor-linked stress converge in common cellular pathways collectively known as integrated stress responses (ISR), which are characterized by the phosphorylation of the eukaryotic translation initiation factor 2 alpha (eIF2α), as well as the induction of the activating transcription factor 4 (Atf4) and the C/EBP homologous protein (Chop; encoded by *Ddit3* and also known as Chop-10 and Gadd153) (Harding et al., 2003; Rzymski and Harris, 2007). Upregulation of Chop in tumors occurs after chemo- or

NIH-PA Author Manuscript

NIH-PA Author Manuscript

NIH-PA Author Manuscript

radio-therapy or as the result of the uncontrolled growth of malignant cells (Schonthal, 2013), and typically leads to cellular apoptosis (Malhi and Kaufman, 2011). Elevated expression of Chop in tumors correlated with stage, aggressiveness, and low survival in patients with different malignancies (Dalton et al., 2013; Kim et al., 2012). Furthermore, decreased liver carcinoma development was observed in Chop-deficient mice, which associated with reduced amounts of various cytokines (Scaiewicz et al., 2013; zwaan-McCabe et al., 2013). An initial report suggested the role of stress-linked responses on the function of MDSCs (Condamine et al., 2014). However, the specific role of Chop in the modulation of anti-tumor immunity remains unknown.

We aimed to determine the role of tumor-stromal Chop in the suppression of immune responses in tumor-bearing hosts. Our results demonstrate the critical role of Chop in the accumulation and immune regulatory function of MDSCs in tumors. MDSCs lacking Chop had a low capacity to block T cell responses; an impaired expression of major inhibitory pathways; and a high ability to prime T cell function and induce anti-tumor effects. Chop upregulation in MDSCs was mediated by tumor-induced ROS and PNT, and favored the expression of IL-6 and the MDSCs-regulators C/EBPβ and phospho-STAT-3. Also, ectopic expression of IL-6 restored tumor growth and MDSCs activity in Chop-deficient mice. These results show for the first time the checkpoints modulating the interaction between tumor-induced stress and MDSCs in the suppression of anti-tumor immunity and suggest targeting stromal Chop as a means to overcome tumor-induced tolerance and to enhance the efficacy of immunotherapy in cancer.

Results

Expression of Chop in tumor-infiltrating MDSCs regulates tumor growth

The role of Chop in anti-tumor immunity and its distribution within tumor cell populations remains unknown. Therefore, we first compared the expression of Chop in spleens and tumors from mice s.c. injected with 3LL lung carcinoma. An increased expression of Chop was found at the tumor site, compared to the spleen (Figure S1A), and was shared by the malignant cells and infiltrating $CD45^+$ leukocytes (Figure S1B). To identify the distribution of Chop among the tumor-linked leukocytes, we sorted different $CD45^+$ populations from 3LL tumors and monitored their expression of Chop. Higher amounts of Chop were found in MDSCs ($CD11b^+$ $Gr1^+$), compared to other cell populations, including $CD11b^+$ $Gr1^-$ myeloid cells, $CD11b^+$ $CD11c^+$ dendritic cells, $CD11b^+$ $F4/80^+$ macrophages, $B220^+$ B lymphocytes or pDC, and $CD3^+$ T cells (Figure 1A). Moreover, the increased expression of Chop in tumor-linked MDSCs, compared to splenic MDSCs or immature myeloid cells (iMCs), was validated in different tumor models, including 3LL, B16 (melanoma), EL-4 (thymoma), and MCA-38 (colon carcinoma) (Figure 1B); and correlated with the MDSCs ability to block T cell proliferation (Figure S1C). Next, we tested if human MDSCs infiltrating tumors displayed an increased expression of Chop. Using a panel of colon carcinoma samples, we found a preferential Chop upregulation in $CD33^+$ myeloid cells, which were found in minimal numbers in normal colon tissues (Figure 1C, Figure S1D). In addition, Chop expression in colon tumors was restricted to $CD66b^+$ $HLA\text{-}DR^-$ populations

NIH-PA Author Manuscript

NIH-PA Author Manuscript

NIH-PA Author Manuscript

(Figure 1D) (Talmadge and Gabrilovich, 2013), demonstrating the expression of Chop in human MDSCs.

To determine the effect of stromal Chop in tumor growth, C57BL/6 controls and Chop-deficient mice (referred as *Ddit3*$^{-/-}$) were injected s.c. with different tumors carrying functional Chop, after which tumor growth kinetics and survival were monitored. In all tested tumor models, a decreased tumor growth (Figure 1E) and an extended survival (Figure S1E) were noticed in *Ddit3*$^{-/-}$ mice, compared to wild-type controls. In addition, increased tumor cell necrosis and decreased angiogenesis were observed in tumors from *Ddit3*$^{-/-}$ mice (Figure S1F-G). However, endothelial cells (CD31^{+} CD45^{-} CD11b^{-}) sorted from tumors displayed a limited expression of Chop, ruling out a direct effect of Chop in tumor endothelium (Figure S1H). Because MDSCs were the major source of Chop in the tumor stroma, we established their role in the anti-tumor effects found in *Ddit3*$^{-/-}$ mice, using a bone marrow (BM) chimeric model (Loinard et al., 2012). Briefly, lethally irradiated CD45.1^{+} mice were reconstituted with BM cells isolated from CD45.2^{+} *Ddit3*$^{-/-}$ mice or controls. Additionally, lethally irradiated CD45.2^{+} *Ddit3*$^{-/-}$ mice were transplanted with CD45.1^{+} wild type BM cells. Greater than 90% chimerism (Figure S1I-J) and equal numbers of CD11b^{+} Gr1^{+} cells (data not shown) were found in all conditions 7 weeks post-transplant. A similar delay in tumor growth was found in *Ddit3*$^{-/-}$ BM chimeric mice and systemic *Ddit3*$^{-/-}$ mice, as compared to controls (Figure 1F). In addition, reconstitution of *Ddit3*$^{-/-}$ mice with wild type BM resulted in a similar tumor growth as that observed in wild type controls (Figure 1F), suggesting the key role of MDSCs-linked Chop in tumor growth. To further demonstrate the role of MDSCs in the anti-tumor effects found in *Ddit3*$^{-/-}$ mice, we depleted MDSCs by treatment with anti-Gr1 antibodies (Mundy-Bosse et al., 2011). Pharmacological depletion of MDSCs induced anti-tumor effects in wild type mice, while it resulted in a partial recovery of tumor growth in 3LL-bearing *Ddit3*$^{-/-}$ mice (Figure 1G), suggesting the functional difference between MDSCs from tumor-bearing wild type and *Ddit3*$^{-/-}$ mice. Thus, our results suggest that tumor-MDSC display a preferential increased expression of Chop and that deletion of Chop induced anti-tumor effects in a MDSCs-dependent manner.

Chop regulates the proliferation, turnover, and immune inhibitory activity of MDSCs

We tested the impact of Chop in the accumulation, turnover, and immune inhibitory function of MDSCs. Similar percentages of MDSCs were found in the spleen and BM of wild type and *Ddit3*$^{-/-}$ mice with and without tumors (Figure S2A-B). In contrast, an elevated percentage of MDSCs was detected in tumors from *Ddit3*$^{-/-}$ mice, compared to controls, with both G-MDSCs and M-MDSCs showing increases (Figure 2A). Interestingly, the accumulation of tumor-MDSCs in *Ddit3*$^{-/-}$ mice did not extend to other myeloid populations, such as DCs (CD11b^{+} Gr1^{-}CD11c^{+}) and macrophages (CD11b^{+} Gr1^{-} F4/80^{+}) (Figure S2C-D). To test the specific role of Chop in MDSCs accumulation in tumors, BM-MDSCs were harvested from 3LL-bearing wild type and *Ddit3*$^{-/-}$ mice, labeled with high and low concentrations of CFSE, mixed in a 1:1 ratio, and adoptively transferred into wild type mice bearing 3LL cells. After 24 hours of transfer, we found similar amounts of transferred wild type and *Ddit3*$^{-/-}$ MDSCs in spleen, while higher numbers of *Ddit3*$^{-/-}$ MDSCs were noted in tumors (Figure 2B). To further understand the increased

NIH-PA Author Manuscript

NIH-PA Author Manuscript

NIH-PA Author Manuscript

accumulation of *Ddit3*$^{-/-}$ MDSCs in tumors, we investigated the effect of Chop in the proliferation and decay of MDSCs. A similar proliferation of spleen and bone marrow MDSCs was found in wild type and *Ddit3*$^{-/-}$ mice, as tested by BrdU uptake (Figure S2E-F). In contrast, an elevated tumor-MDSCs proliferation was noted in *Ddit3*$^{-/-}$ mice, compared to controls (Figure 2C). Moreover, decreased expression of the apoptosis markers, annexin V and cleaved caspase 3 (Figure 2D), were detected in tumor-MDSCs from *Ddit3*$^{-/-}$ mice, compared to wild type MDSCs. Thus, Chop deletion increased proliferation and reduced turnover of tumor-MDSCs.

We then asked whether Chop deletion affected the immune inhibitory ability of MDSCs. Tumor-sorted MDSCs from *Ddit3*$^{-/-}$ mice had a reduced capacity to block activated T cell proliferation and IFNγ production, as compared to those from control mice (Figure 2E). A similar decreased inhibitory function was also detected in MDSCs from tumor-bearing *Ddit3*$^{-/-}$ BM chimeras (Figure 2F). Interestingly, the low regulatory potential of *Ddit3*$^{-/-}$ MDSCs correlated with an impaired synthesis of major molecules linked to MDSCs activity, including arginase I, PNT, and superoxide; but an increased iNOS expression (Figure 2G). To test the role of Chop in the tolerogenic activity of MDSCs *in vivo*, CD45.2^{+} anti-$OVA_{257-264}$ (SIINFEKL) transgenic CD8^{+} OT-1 cells were adoptively transferred into CD45.1^{+} mice, followed by immunization with wild type DCs loaded with SIINFEKL. Tumor-MDSCs from wild type or *Ddit3*$^{-/-}$ mice pulsed with SIINFEKL were transferred the same day of immunization, as well as 5 days later (Dolcetti et al., 2010). Transferred MDSCs had a similar low contamination with CD11c^{+} DCs and F4/80^{+} macrophages (Figure S2G-I). Twelve days after vaccination, lymph nodes were harvested, challenged with SIINFEKL, and tested for IFNγ production by Elispot. A significant decrease in the production of IFNγ was found in mice transferred with SIINFEKL-loaded DCs and wild type MDSCs (Figure 2H). Conversely, transfer of *Ddit3*$^{-/-}$ MDSCs further enhanced the numbers of IFNγ^{+} cells induced by the SIINFEKL-DCs vaccine, suggesting that Chop deletion not only blocked the tolerogenic activity of MDSCs, but also allowed MDSCs to increase T cell function.

Chop deficient MDSCs induce anti-tumor responses and prime T cell proliferation

We hypothesized that deletion of Chop in MDSCs enables them to induce anti-tumor responses. Thus, 3LL cells were mixed 1:1 with MDSCs isolated from wild type or *Ddit3*$^{-/-}$ mice bearing 3LL tumors and injected s.c. into wild type or *Ddit3*$^{-/-}$ mice. Co-injection of *Ddit3*$^{-/-}$ MDSCs into wild type mice significantly delayed tumor growth, whereas co-injection of wild type MDSCs into *Ddit3*$^{-/-}$ mice partially restored tumor growth (Figure 3A). We next evaluated the therapeutic effect of *Ddit3*$^{-/-}$ MDSCs in established tumors. Adoptive transfer of *Ddit3*$^{-/-}$ MDSCs after 3 and 6 days of 3LL injection delayed tumor growth, while transfer of wild type MDSCs accelerated 3LL growth (Figure 3B). A possible explanation for these results could be that *Ddit3*$^{-/-}$ MDSCs directly killed tumor cells. However, a low anti-tumor cytotoxicity was displayed by wild type and *Ddit3*$^{-/-}$ MDSCs (Figure 3C), ruling out a direct anti-tumor effect of *Ddit3*$^{-/-}$ MDSCs. Alternatively, we tested whether Chop deletion allowed MDSCs to prime T cell responses. Thus, MDSCs were sorted from wild type and *Ddit3*$^{-/-}$ mice bearing 3LL tumors, after which they were loaded with SIINFEKL, washed, and co-cultured with CFSE-labeled naïve OT-1 cells. A

NIH-PA Author Manuscript

NIH-PA Author Manuscript

NIH-PA Author Manuscript

higher proliferation was observed in OT-1 cells co-cultured with *Ddit3*$^{-/-}$ MDSCs, compared to those co-cultured with wild type MDSCs (Figure 3D), suggesting that Chop deletion enabled MDSCs to induce T cell proliferation. In fact, *Ddit3*$^{-/-}$ MDSCs displayed a higher expression of major histocompatibility complex (MHC) class I and II (Figure 3E). Thus, Chop deficient MDSCs induced anti-tumor effects and had the ability to activate T cells responses.

Chop in MDSCs is a central mediator of tumor-induced tolerance

We then determined whether the deletion of stromal Chop impacted the suppression of T cell responses in tumors. We found in tumor-bearing *Ddit3*$^{-/-}$ mice an increased infiltration of CD45^{+} cells (Figure S3) and CD8^{+} T cells in the tumors (Figure 4A), and an elevated number of CD8^{+} T cells producing IFNγ after activation (Figure 4B). Furthermore, a partial recovery of CD3ζ chain expression, a key protein for T cell activation, was observed in T cells from 3LL-bearing *Ddit3*$^{-/-}$ mice, compared to those from controls with tumors (Figure 4C). Although T cells infiltrating tumors were negative for Chop expression (Figure 1A), we tested their effect as mediators of the anti-tumor responses found in *Ddit3*$^{-/-}$ mice. Depletion of CD8^{+} T cells, but not CD4^{+} T cells, restored tumor growth in 3LL-bearing *Ddit3*$^{-/-}$ mice (Figure 4D), suggesting a potential role of CD8^{+} T cells in the anti-tumor responses induced by Chop deletion.

To address the role of Chop in tumor-induced tolerance, wild type and *Ddit3*$^{-/-}$ mice (CD45.2^{+}) were injected s.c. with 3LL tumors expressing the model tumor antigen ovalbumin (OVA). Seven days later, 5×10^{6} CD45.1^{+} CD8^{+} OT-1 cells were adoptively transferred into the mice, followed by vaccination with SIINFEKL. A higher anti-tumor effect was noted in *Ddit3*$^{-/-}$ mice receiving OT-1 cells, as compared to wild type controls transferred with the same number of T cells (Figure 4E). In addition, elevated numbers of T cells producing IFNγ were detected in the spleens of vaccinated tumor-bearing *Ddit3*$^{-/-}$ mice after activation *ex vivo* with SIINFEKL (Figure 4F), which correlated with a higher total yield of transferred CD45.1^{+} OT-1 cells in both the spleens and tumors (Figure 4G). Because these results could be explained by a low suppression driven by the smaller tumors observed in *Ddit3*$^{-/-}$ mice, we repeated the experiment in wild type and *Ddit3*$^{-/-}$ mice bearing similar sized 3LL-OVA tumors (~100 mm^{3}, day 8 for wild type and day 15 for *Ddit3*$^{-/-}$ mice). An increased production of IFNγ^{+} after SIINFEKL activation (Figure 4H) and higher numbers of CD45.1^{+} OT-1 T cells in the spleens and tumors (Figure 4I) were detected in tumor-bearing *Ddit3*$^{-/-}$ mice, compared to controls, suggesting the key role of Chop in tumor-induced tolerance and the potential benefit of its deletion for T cell-based immunotherapy.

Mediators of Chop expression in MDSCs

We investigated the role of the tumor environment in the induction of Chop in MDSCs and the effect of Chop in the promotion of MDSCs function by tumors. BM-MDSCs (Marigo et al., 2010) were treated with 3LL tumor explant supernatants (TES), after which MDSCs were tested for the induction of Chop and the ability to block T cell proliferation. TES treatment induced Chop expression in MDSCs (Figure 5A) and increased MDSCs-regulatory activity (Figure 5B). Interestingly, *Ddit3*$^{-/-}$ BM-MDSCs failed to increase

NIH-PA Author Manuscript

NIH-PA Author Manuscript

NIH-PA Author Manuscript

inhibitory function after TES treatment (Figure 5B), suggesting the role of Chop in the regulation of MDSCs function by tumors. To identify the major mediators leading to the expression of Chop in MDSCs, we initially tested the effect of ROS and PNT. Higher amounts of PNT and ROS were found in tumors, compared to spleens of 3LL-bearing mice and controls (Figure S4A-B); and in tumor-MDSCs compared to spleen MDSCs and iMCs (Figure S4C-D). In addition, treatment of BM-MDSCs with PNT, and to a lesser extent with H_2O_2, led to a similar induction of Chop as that induced by TES (Figure 5C). In agreement with these data, inhibition of Chop upregulation was noted in TES-treated BM-MDSCs after the addition of antioxidant N-acetyl cysteine (L-NAC) and PNT scanvenger MNTBAP, but not nitric oxide scavenger PTIO (Figure 5D). Moreover, treatment of tumor-bearing mice with L-NAC resulted in a lower expression of Chop in tumor-MDSCs (Figure 5E); and a similar effect as that induced by Chop deletion, including a delayed tumor growth (Figure 5F, Figure S4E), an impaired MDSCs inhibitory function (Figure 5G), and reduced levels of arginase I (Figure 5E). Because MDSCs were a major source of PNT in tumors (Figure 5H), we aimed to determine if the endogenous production of ROS or PNT in MDSCs modulated Chop. Deletion of $Gp91^{phox}$, a key component in the production of ROS and PNT by MDSCs (Corzo et al., 2009), blocked Chop upregulation in TES-treated BM-MDSCs (Figure 5I), suggesting the endogenous role of ROS or PNT in MDSCs in the induction of Chop by tumors.

Chop expression in MDSCs is mediated by Atf4

ISR are characterized by the expression of phospho-eIF2α and signaling through Atf4 protein. We aimed to determine the role of ISR in the induction of Chop in MDSCs. Increased expression of phospho-eIF2α and Atf4 were noted in MDSCs from tumors and TES treated-BM-MDSCs (Figure 6A). Furthermore, the elevated expression of Chop in tumor-linked MDSCs correlated with a higher endogenous binding of Atf4 to Chop promoter, as tested by ChIP assays (Figure 6B). To confirm the role of Atf4 in the induction of Chop in MDSCs from tumors, we used $Atf4^{+/-}$ mice, as $Atf4^{-/-}$ mice showed low survival. Treatment of $Atf4^{+/-}$ BM-MDSCs with TES resulted in an impaired induction of Chop (Figure 6C). In addition, MDSCs isolated from 3LL-bearing $Atf4^{+/-}$ mice showed a 50% decrease in *Atf4* induction (Figure 6D) and a reduction in the expression of Chop (Figure 6E), suggesting the role of Atf4 as a major mediator of Chop induction in MDSCs from tumors. Interestingly, partial deletion of Atf4 triggered a similar anti-tumor effect as that found in $Ddit3^{-/-}$ mice (Figure 6F). Thus, the induction of Chop in tumor MDSC was mediated by induction of Atf4.

Chop regulates MDSCs activity by modulating IL-6

We sought to understand the mechanisms by which the deletion of Chop impaired MDSCs function. Previous studies showed the role of C/EBPβ in MDSCs function (Marigo et al., 2010); and Chop in C/EBPβ activity (Hattori et al., 2003). Thus, we hypothesized that Chop deletion impaired C/EBPβ signaling in MDSCs. Similar levels of C/EBPβ mRNA were found in wild type and $Ddit3^{-/-}$ MDSCs from tumors (Figure 7A). Conversely, a higher expression of the inhibitory form C/EBPβ LIP, without changes in C/EBPβ LAP and LAP*, was found in $Ddit3^{-/-}$ MDSCs, compared to controls (Figure 7A). A similar elevation of C/EBPβ LIP was also noted in MDSCs from L-NAC-treated mice, suggesting the role of ROS

NIH-PA Author Manuscript

NIH-PA Author Manuscript

NIH-PA Author Manuscript

or PNT as mediators of this pathway (Figure 7B). Translation of C/EBPβ LIP in MDSCs is favored by the expression of micro-RNA 142-3p (miR-142-3p)(Sonda et al., 2013). Accordingly, higher levels of miR-142-3p were detected in *Ddit3*$^{-/-}$ MDSCs, compared to controls (Figure 7C). Furthermore, *Ddit3*$^{-/-}$ MDSCs had decreased C/EBPβ activity, as tested by DNA-binding ELISA (Figure 7D); and inhibited endogenous binding of C/EBPβ to IL-6 and arginase I promoters, measured by ChIP assay (Figure 7E). The reduced binding of C/EBPβ to IL-6 promoter in *Ddit3*$^{-/-}$ MDSCs translated into a decreased production of IL-6 (Figure 7F) and lower expression of IL-6 receptor-linked protein, phospho-STAT3 (Figure 7G). However, similar expression of IL-6 receptors gp126 and gp130 (Figure S5A) in tumor-MDSCs and equal induction of phospho-STAT3 in response to exogenous IL-6 (Figure S5B) were found in wild type and *Ddit3*$^{-/-}$ MDSCs, suggesting that a decrease in IL-6 rather than a low sensitivity to IL-6 was modulated by Chop knockdown.

To determine the significance of the low expression of IL-6 in the anti-tumor effects induced by Chop deletion, 3LL cells over expressing IL-6 (3LL-*IL-6*) were injected into wild type and *Ddit3*$^{-/-}$ mice. Ectopic expression of IL-6 restored tumor growth in *Ddit3*$^{-/-}$ mice (Figure 7H). In addition, MDSCs from *Ddit3*$^{-/-}$ mice bearing 3LL-*IL-6* tumors were equally suppressive as control MDSCs from 3LL or 3LL-*IL-6*-bearing mice (Figure 7I). Furthermore, the decreased levels of phospho-STAT3 observed in *Ddit3*$^{-/-}$ MDSCs were partially restored after ectopic expression of IL-6 in tumors cells (Figure 7J). These suggest the relevance of IL-6 in the anti-tumor effects induced by MDSCs-Chop deletion.

Discussion

Although an adequate ISR in tumor cells is fundamental for their growth and survival *in vivo* (Rouschop et al., 2010; Ye et al., 2010), the biological relevance of ISR in tumor-induced immune suppression remains unknown. In this study, we aimed to determine the interaction between tumor-linked stress and anti-tumor immunity. Our data suggest a new role of Chop as a mediator of tumor-induced anergy through the modulation of MDSCs function and accumulation.

Chop expression is typically associated with pathways leading to cellular apoptosis. In fact, silencing of Chop in tumor cells induced resistance to cell death by various chemotherapy agents (Schonthal, 2013). In addition to its pro-apoptotic effect in tumor cells, Chop also regulated cell death processes in primary myeloid populations. Deletion of Chop decreased apoptosis in liver and fat tissue macrophages from mice exposed to high fat diet (Grant et al., 2014; Malhi et al., 2013). Moreover, low numbers of apoptotic CD11b^{+} cells were found in the intestinal mucosa of *Ddit3*$^{-/-}$ mice undergoing colitis, which correlated with a decreased disease progression (Namba et al., 2009). We show that Chop deletion inhibited MDSCs turnover, but also changed MDSCs-immune suppressive function into one that promotes anti-tumoral T cell responses, suggesting the role of Chop as a central mediator of the inflammatory function in MDSCs. Accordingly, low levels of MDSCs-linked cytokines were detected in *Ddit3*$^{-/-}$ mice having spontaneous liver carcinomas (Scaiewicz et al., 2013; zwaan-McCabe et al., 2013). Moreover, *Ddit3*$^{-/-}$ mice were protected against inflammatory damage after lipopolysaccharide (LPS)-induced lung injury (Endo et al., 2006). In contrast to our results, previous studies suggested an increased tumor node formation in *Ddit3*$^{-/-}$

NIH-PA Author Manuscript

NIH-PA Author Manuscript

NIH-PA Author Manuscript

mice and increased kidney inflammation after LPS-induced kidney injury (Esposito et al., 2013; Huber et al., 2013). These opposite results could be explained by a differential role of MDSCs in particular inflammation models and the potential expression of Chop in other cell populations, including tumor cells. Previous studies showed the upregulation of Chop in T cells co-cultured with IDO-expressing pDC (Munn et al., 2005). Unexpectedly, although T cells were the ultimate mediators of the anti-tumor responses induced by Chop deletion, we did not detect significant levels of Chop in tumor-linked T cells. However, we do not discard a potential direct effect of Chop on T cells under specific stress-related conditions.

Inflammatory function of MDSCs is highly dependent on C/EBPβ and phospho-STAT3 (Sonda et al., 2011). C/EBPβ LAP and LAP* are major transcriptional activators of IL-6 (Hattori et al., 2003), while IL-6 plays a major role in the induction of phospho-STAT3 (Schafer and Brugge, 2007). We found a preferential expression of C/EBPβ inhibitory form LIP in *Ddit3*$^{-/-}$ MDSCs, which correlated with low levels of IL-6 and phospho-STAT3. This suggests the upstream role of Chop in the regulation of master MDSCs mediators. A recent study showed the regulation of IL-6 by Chop in LPS-treated macrophages (Liu et al., 2013). Our results show the critical role of the decrease in IL-6 in the anti-tumor effects induced by Chop deletion. However, the effect of LIP in the low IL-6 production found in *Ddit3*$^{-/-}$ MDSCs and the pathways by which Chop deletion leads to LIP upregulation remain unknown. The specific translation of C/EBPβ LAP, LAP*, or LIP in MDSCs is regulated by the expression of miR-142-3p (Sonda et al., 2013), which was upregulated in *Ddit3*$^{-/-}$ MDSCs. Therefore, a potential interaction between Chop and miR-142-3p could be responsible for the increased expression of LIP in *Ddit3*$^{-/-}$ MDSCs.

A major question is how MDSCs express Chop without completely undergoing apoptosis. Atf4 induction by cellular stress is associated with pathways maintaining survival, whereas Chop is mostly linked to stress-induced cell death. The interaction of pro-survival pathways induced by Atf4 and pro-apoptotic signaling linked to Chop is regulated by miR-211, which transiently prevents Chop transcription (Chitnis et al., 2012). However, it is unknown if miR-211 plays a role in MDSCs function and turnover. Induction of Chop in MDSCs was mediated by Atf4 and correlated with phosphorylation of eIF2α. Phospho-eIF2α is induced by the double-stranded RNA-dependent kinase (Pkr), hemin-regulated inhibitor kinase (Hri), PKR-like ER related kinase (Perk), and general control non-repressed 2 kinase (Gcn2). Exposure of tumor cells to high levels of ROS led to endoplasmic reticulum (ER) stress, activation of Perk, and induction of Chop (Harding et al., 2003; vivar-Valderas et al., 2011). Furthermore, induction of ER stress in tumor cells promoted the expression of chronic inflammatory mediators in myeloid cells (Mahadevan et al., 2011). Interestingly, Perk deletion in tumor cells prevented tumor growth, which correlated with low inflammation and sensitivity to stress mediators (Bi et al., 2005; Bobrovnikova-Marjon et al., 2010; Hart et al., 2012). However, the effect of ER stress and Perk in MDSCs function remains to be identified. Initial findings suggest the role of ER stress in the modulation of MDSCs survival through expression of DR5 (Condamine et al., 2014). Chop induction, especially by starvation-mediated mechanisms could also be mediated through Gcn2. Therefore, understanding the role of eIF2α kinases in the induction of Chop in MDSCs is critical to determine the effect of tumor stress in anti-tumor immunity.

NIH-PA Author Manuscript

NIH-PA Author Manuscript

NIH-PA Author Manuscript

Although there are no current therapies to block Chop, some therapeutic possibilities could include the inhibition or scavenging of ROS and/or PNT (Bronte et al., 2005; Corzo et al., 2009; De et al., 2005; Lu et al., 2011; Sawant et al., 2013). Indeed, treatment with L-NAC reduced tumor growth and blocked Chop expression in MDSCs. Thus, further investigation of the links between tumor-linked stress and ISR checkpoints are expected to enable the therapeutic inhibition of Chop. In summary, our data demonstrate the central role of Chop in MDSCs suppressive activity and suggest the feasibility of overcoming tumor-induced MDSCs suppression by blocking Chop.

Experimental Procedures

Mice and Cell lines

C57BL/6 mice (6 to 8-wk-old female) were obtained from Harlan (Indianapolis, IN). *Ddit3*$^{-/-}$, *Gp91*$^{phox-/-}$, and *Atf4*$^{+/-}$ mice were purchased from the Jackson Laboratories (Bar Harbor, ME). 3LL lung carcinoma, B16 melanoma, MCA-38 colon carcinoma, and EL-4 thymoma cells (American Type Culture Collection, Manassas, VA) were injected s.c. into the mice and tumor volume measured and calculated using the formula [(small diameter)^2 × (large diameter) × 0.5]. Experiments using animals were approved by the LSU-IACUC and were performed following LSU animal care facility guidelines. Ovalbumin or IL-6-expressing 3LL cells (3LL-OVA, or 3LL-*IL-6*) were generated by transfection using Lipofectamine 2000 (Life Technologies) with vectors coding for cytosolic chicken ovalbumin or IL-6, and harboring a neomycin resistance cassette (Addgene). Single 3LL clones were selected in medium supplemented with 500 μg/ml Geneticin. BM-MDSCs were generated by culturing BM cells for 3 days in the presence of G-CSF (100 ng/mL) and GM-CSF (20 ng/mL). For MDSCs depletion, 200 μg anti-Gr-1 antibody (clone RB6-8C5, BioXcell) was administered i.p. on day 0 and every 4th day until endpoint. For CD4$^+$ or CD8$^+$ T cell depletion studies, mice were pre-treated 24 hours before tumor injection with 400 μg anti-CD4 (clone GK1.5) or anti-CD8 (clone 53.6.72). Maintenance doses of the depleting antibodies were given twice a week. Cytotoxic effects of tumor MDSC on 3LL cells *in vitro* were determined by non-radioactive cytotoxicity assay using LDH (Promega, Madison, WI). L-NAC (1 mg/kg/day) was injected i.p. starting at day 1 post-tumor injection.

Antibodies

The detailed list of the used antibodies is available in the Supplementary methods.

Bone Marrow Chimeras

Recipient mice lethally irradiated with 950 rads were reconstituted with 1 × 10^7 BM cells and 1 × 10^6 splenocytes from donor mice. Chimeric engraftment was verified in peripheral blood 7 weeks after transplantation by monitoring the corresponding switch from CD45.1$^+$ cells into CD45.2$^+$ or from CD45.2$^+$ into CD45.1$^+$ using flow cytometry. A week later, mice were injected s.c. with 3LL tumor cells.

Tolerogenic effect of MDSCs

CD8$^+$ T cells (5 × 10^6) from CD45.2$^+$ OT-1 mice were adoptively transferred into CD45.1$^+$ mice. Two days later MDSCs were sorted from 3LL tumor-bearing wild type or *Ddit3*$^{-/-}$

NIH-PA Author Manuscript

NIH-PA Author Manuscript

NIH-PA Author Manuscript

mice, pulsed with 2 μg/mL SIINFEKL for 1 hour, and 5×10^6 MDSCs transferred i.v. into the mice previously injected with OT-1. The same day, mice received s.c. vaccination with 4×10^6 DCs generated from BM cultured for 6 days in media containing GM-CSF (20 ng/mL) and IL-4 (10 ng/mL). During the final 24 hours of culture, DCs were exposed to 2 μg/mL SIINFEKL and 1μg/mL LPS. Mice received a second injection with SIINFEKL-pulsed MDSCs 5 days later. Twelve days after the initial DCs immunization, draining lymph nodes were recovered and challenge with SIINFEKL for 24 hours, after which they were monitored for IFNγ production by Elispot (R & D systems).

Adoptive Cellular therapy

$CD45.2^+$ wild type or *Ddit3*$^{-/-}$ mice were injected with 3LL-OVA cells (1×10^6) at day 0 or at stratified time points to achieve tumor of similar palpable volume. Mice then received adoptive transfer of 5×10^6 $CD45.1^+$ $CD8^+$ OT-1 cells via tail vein. The following day, mice were vaccinated s.c. with 100 μg of SIINFEKL peptide in 0.2 mL of PBS. Ten days later, spleens and tumors were tested for transferred OT-1 cells and function.

IL-6 production in MDSCs

For analysis of IL-6 production in MDSCs, tumor-bearing mice were injected i.p. with 0.25 mg of Brefeldin A for 6 hours, after which tumors were isolated and MDSCs tested for IL-6 by flow cytometry. To assess IL-6 signaling, BM-MDSCs were developed using BM cells from wild type, and *Ddit3*$^{-/-}$ mice. On protocol day 3, recombinant mouse IL-6 (R&D Systems) was supplemented to the culture at 50 ng/mL for 8 hours.

MDSCs suppressive mechanism assays

Superoxide production was quantified in freshly isolated MDSCs using the Superoxide Anion Assay Kit (Sigma). Peroxynitrite levels were determined in tissue or MDSCs lysates using a Nitrotyrosine ELISA Assay (EMD Millipore).

C/EBPβ activity

Nuclear extracts from MDSCs were tested for C/EBPβ DNA binding activity using the TransAM C/EBPβ DNA-binding ELISA kit (Active Motif, Carlsbad, CA).

Supplementary Material

Refer to Web version on PubMed Central for supplementary material.

Acknowledgments

We thank the Immunology Core Laboratories from the Stanley S. Scott Cancer Center (LSU-HSC) and Tulane University (funded through P20GM103501 and P20GM103518, respectively) for their help with the flow sorting studies.

Financial support: This work was supported in part by National Institutes of Health (NIH) grant P20GM103501 subproject #3 to P.C.R., and NIH-R21CA162133 to P.C.R.

NIH-PA Author Manuscript

NIH-PA Author Manuscript

NIH-PA Author Manuscript

Abbreviations

Atf4	Activating-transcription factor 4
Chop	C/EBP Homologous Protein
C/EBPβ	CCAAT/enhancer-binding protein-β
LAP* and LAP	C/EBPβ liver-enriched activator proteins
LIP	C/EBPβ liver-enriched inhibitory protein
eIF2α	Eukaryotic translation initiation factor 2 alpha
ISR	integrated stress responses
IL-6	Interleukin-6
MDSCs	Myeloid-derived suppressor cells
PNT	peroxynitrite
ROS	Reactive oxygen species
STAT3	Signal transducer of activator of transcription 3

Reference List

Bi M, Naczki C, Koritzinsky M, Fels D, Blais J, Hu N, Harding H, Novoa I, Varia M, Raleigh J, et al. ER stress-regulated translation increases tolerance to extreme hypoxia and promotes tumor growth. EMBO J. 2005; 24:3470–3481. [PubMed: 16148948]

Bobrovnikova-Marjon E, Grigoriadou C, Pytel D, Zhang F, Ye J, Koumenis C, Cavener D, Diehl JA. PERK promotes cancer cell proliferation and tumor growth by limiting oxidative DNA damage. Oncogene. 2010; 29:3881–3895. [PubMed: 20453876]

Bronte V, Kasic T, Gri G, Gallana K, Borsellino G, Marigo I, Battistini L, Iafrate M, Prayer-Galetti T, Pagano F, et al. Boosting antitumor responses of T lymphocytes infiltrating human prostate cancers. J.Exp.Med. 2005; 201:1257–1268. [PubMed: 15824085]

Chen DS, Mellman I. Oncology meets immunology: the cancer-immunity cycle. Immunity. 2013; 39:1–10. [PubMed: 23890059]

Chitnis NS, Pytel D, Bobrovnikova-Marjon E, Pant D, Zheng H, Maas NL, Frederick B, Kushner JA, Chodosh LA, Koumenis C, et al. miR-211 is a prosurvival microRNA that regulates chop expression in a PERK-dependent manner. Mol.Cell. 2012; 48:353–364. [PubMed: 23022383]

Condamine T, Kumar V, Ramachandran IR, Youn JI, Celis E, Finnberg N, El-Deiry WS, Winograd R, Vonderheide RH, English NR, et al. ER stress regulates myeloid-derived suppressor cell fate through TRAIL-R-mediated apoptosis. J.Clin.Invest. 2014; 124:2626–2639. [PubMed: 24789911]

Corzo CA, Cotter MJ, Cheng P, Cheng F, Kusmartsev S, Sotomayor E, Padhya T, McCaffrey TV, McCaffrey JC, Gabrilovich DI. Mechanism regulating reactive oxygen species in tumor-induced myeloid-derived suppressor cells. J.Immunol. 2009; 182:5693–5701. [PubMed: 19380816]

Coussens LM, Zitvogel L, Palucka AK. Neutralizing tumor-promoting chronic inflammation: a magic bullet? Science. 2013; 339:286–291. [PubMed: 23329041]

Dalton LE, Clarke HJ, Knight J, Lawson MH, Wason J, Lomas DA, Howat WJ, Rintoul RC, Rassl DM, Marciniak SJ. The endoplasmic reticulum stress marker CHOP predicts survival in malignant mesothelioma. Br.J.Cancer. 2013; 108:1340–1347. [PubMed: 23412101]

De SC, Serafini P, Marigo I, Dolcetti L, Bolla M, Del SP, Melani C, Guiducci C, Colombo MP, Iezzi M, et al. Nitroaspirin corrects immune dysfunction in tumor-bearing hosts and promotes tumor eradication by cancer vaccination. Proc.Natl.Acad.Sci.U.S.A. 2005; 102:4185–4190. [PubMed: 15753302]

NIH-PA Author Manuscript

NIH-PA Author Manuscript

NIH-PA Author Manuscript

Descombes P, Schibler U. A liver-enriched transcriptional activator protein, LAP, and a transcriptional inhibitory protein, LIP, are translated from the same mRNA. Cell. 1991; 67:569–579. [PubMed: 1934061]

Dolcetti L, Peranzoni E, Bronte V. Measurement of myeloid cell immune suppressive activity. Curr.Protoc.Immunol. 2010 *Chapter 14*, Unit.

Endo M, Mori M, Akira S, Gotoh T. C/EBP homologous protein (CHOP) is crucial for the induction of caspase-11 and the pathogenesis of lipopolysaccharide-induced inflammation. J.Immunol. 2006; 176:6245–6253. [PubMed: 16670335]

Esposito V, Grosjean F, Tan J, Huang L, Zhu L, Chen J, Xiong H, Striker GE, Zheng F. CHOP deficiency results in elevated lipopolysaccharide-induced inflammation and kidney injury. Am.J.Physiol Renal Physiol. 2013; 304:F440–F450. [PubMed: 23235477]

Gabrilovich DI, Ostrand-Rosenberg S, Bronte V. Coordinated regulation of myeloid cells by tumours. Nat.Rev.Immunol. 2012; 12:253–268. [PubMed: 22437938]

Grant RW, Nguyen KY, Ravussin A, Albarado D, Youm YH, Dixit VD. Inactivation of C/ebp homologous protein driven immune-metabolic interactions exacerbate obesity and adipose tissue leukocytosis. J.Biol.Chem. 2014

Harding HP, Zhang Y, Zeng H, Novoa I, Lu PD, Calfon M, Sadri N, Yun C, Popko B, Paules R, et al. An integrated stress response regulates amino acid metabolism and resistance to oxidative stress. Mol.Cell. 2003; 11:619–633. [PubMed: 12667446]

Hart LS, Cunningham JT, Datta T, Dey S, Tameire F, Lehman SL, Qiu B, Zhang H, Cerniglia G, Bi M, et al. ER stress-mediated autophagy promotes Myc-dependent transformation and tumor growth. J.Clin.Invest. 2012; 122:4621–4634. [PubMed: 23143306]

Hattori T, Ohoka N, Hayashi H, Onozaki K. C/EBP homologous protein (CHOP) up-regulates IL-6 transcription by trapping negative regulating NF-IL6 isoform. FEBS Lett. 2003; 541:33–39. [PubMed: 12706815]

Huber AL, Lebeau J, Guillaumot P, Petrilli V, Malek M, Chilloux J, Fauvet F, Payen L, Kfoury A, Renno T, et al. p58(IPK)-mediated attenuation of the proapoptotic PERK-CHOP pathway allows malignant progression upon low glucose. Mol.Cell. 2013; 49:1049–1059. [PubMed: 23395000]

Kim KM, Yu TK, Chu HH, Park HS, Jang KY, Moon WS, Kang MJ, Lee DG, Kim MH, Lee JH, et al. Expression of ER stress and autophagy-related molecules in human non-small cell lung cancer and premalignant lesions. Int.J.Cancer. 2012; 131:E362–E370. [PubMed: 21953091]

Liu H, Huang L, Bradley J, Liu K, Bardhan K, Ron D, Mellor AL, Munn DH, McGaha TL. GCN2 dependent metabolic stress is essential for cytokine induction and pathology in murine sepsis. Mol.Cell Biol. 2013

Loinard C, Zouggari Y, Rueda P, Ramkhelawon B, Cochain C, Vilar J, Recalde A, Richart A, Charue D, Duriez M, et al. C/EBP homologous protein-10 (CHOP-10) limits postnatal neovascularization through control of endothelial nitric oxide synthase gene expression. Circulation. 2012; 125:1014–1026. [PubMed: 22265908]

Lu T, Ramakrishnan R, Altiok S, Youn JI, Cheng P, Celis E, Pisarev V, Sherman S, Sporn MB, Gabrilovich D. Tumor-infiltrating myeloid cells induce tumor cell resistance to cytotoxic T cells in mice. J.Clin.Invest. 2011; 121:4015–4029. [PubMed: 21911941]

Mahadevan NR, Rodvold J, Sepulveda H, Rossi S, Drew AF, Zanetti M. Transmission of endoplasmic reticulum stress and pro-inflammation from tumor cells to myeloid cells. Proc.Natl.Acad.Sci.U.S.A. 2011; 108:6561–6566. [PubMed: 21464300]

Malhi H, Kaufman RJ. Endoplasmic reticulum stress in liver disease. J.Hepatol. 2011; 54:795–809. [PubMed: 21145844]

Malhi H, Kropp EM, Clavo VF, Kobrossi CR, Han J, Mauer AS, Yong J, Kaufman RJ. C/EBP homologous protein-induced macrophage apoptosis protects mice from steatohepatitis. J.Biol.Chem. 2013; 288:18624–18642. [PubMed: 23720735]

Marigo I, Bosio E, Solito S, Mesa C, Fernandez A, Dolcetti L, Ugel S, Sonda N, Bicciato S, Falisi E, et al. Tumor-induced tolerance and immune suppression depend on the C/EBPbeta transcription factor. Immunity. 2010; 32:790–802. [PubMed: 20605485]

Movahedi K, Guilliams M, Van den BJ, Van den BR, Gysemans C, Beschin A, De BP, Van Ginderachter JA. Identification of discrete tumor-induced myeloid-derived suppressor cell

NIH-PA Author Manuscript

NIH-PA Author Manuscript

NIH-PA Author Manuscript

subpopulations with distinct T cell-suppressive activity. Blood. 2008; 111:4233–4244. [PubMed: 18272812]

Mundy-Bosse BL, Lesinski GB, Jaime-Ramirez AC, Benninger K, Khan M, Kuppusamy P, Guenterberg K, Kondadasula SV, Chaudhury AR, La Perle KM, et al. Myeloid-derived suppressor cell inhibition of the IFN response in tumor-bearing mice. Cancer Res. 2011; 71:5101–5110. [PubMed: 21680779]

Munn DH, Sharma MD, Baban B, Harding HP, Zhang Y, Ron D, Mellor AL. GCN2 kinase in T cells mediates proliferative arrest and anergy induction in response to indoleamine 2,3-dioxygenase. Immunity. 2005; 22:633–642. [PubMed: 15894280]

Namba T, Tanaka K, Ito Y, Ishihara T, Hoshino T, Gotoh T, Endo M, Sato K, Mizushima T. Positive role of CCAAT/enhancer-binding protein homologous protein, a transcription factor involved in the endoplasmic reticulum stress response in the development of colitis. Am.J.Pathol. 2009; 174:1786–1798. [PubMed: 19359519]

Pearce EL, Poffenberger MC, Chang CH, Jones RG. Fueling immunity: insights into metabolism and lymphocyte function. Science. 2013; 342:1242454. [PubMed: 24115444]

Raber P, Ochoa AC, Rodriguez PC. Metabolism of L-arginine by myeloid-derived suppressor cells in cancer: mechanisms of T cell suppression and therapeutic perspectives. Immunol.Invest. 2012; 41:614–634. [PubMed: 23017138]

Rouschop KM, van den BT, Dubois L, Niessen H, Bussink J, Savelkouls K, Keulers T, Mujcic H, Landuyt W, Voncken JW, et al. The unfolded protein response protects human tumor cells during hypoxia through regulation of the autophagy genes MAP1LC3B and ATG5. J.Clin.Invest. 2010; 120:127–141. [PubMed: 20038797]

Rzymski T, Harris AL. The unfolded protein response and integrated stress response to anoxia. Clin.Cancer Res. 2007; 13:2537–2540. [PubMed: 17473181]

Sawant A, Schafer CC, Jin TH, Zmijewski J, Tse HM, Roth J, Sun Z, Siegal GP, Thannickal VJ, Grant SC, et al. Enhancement of antitumor immunity in lung cancer by targeting myeloid-derived suppressor cell pathways. Cancer Res. 2013; 73:6609–6620. [PubMed: 24085788]

Scaiewicz V, Nahmias A, Chung RT, Mueller T, Tirosh B, Shibolet O. CCAAT/Enhancer-Binding Protein Homologous (CHOP) Protein Promotes Carcinogenesis in the DEN-Induced Hepatocellular Carcinoma Model. PLoS.One. 2013; 8:e81065. [PubMed: 24339898]

Schafer ZT, Brugge JS. IL-6 involvement in epithelial cancers. J.Clin.Invest. 2007; 117:3660–3663. [PubMed: 18060028]

Schonthal AH. Pharmacological targeting of endoplasmic reticulum stress signaling in cancer. Biochem.Pharmacol. 2013; 85:653–666. [PubMed: 23000916]

Sonda N, Chioda M, Zilio S, Simonato F, Bronte V. Transcription factors in myeloid-derived suppressor cell recruitment and function. Curr.Opin.Immunol. 2011; 23:279–285. [PubMed: 21227670]

Sonda N, Simonato F, Peranzoni E, Cali B, Bortoluzzi S, Bisognin A, Wang E, Marincola FM, Naldini L, Gentner B, et al. miR-142-3p prevents macrophage differentiation during cancer-induced myelopoiesis. Immunity. 2013; 38:1236–1249. [PubMed: 23809164]

Talmadge JE, Gabrilovich DI. History of myeloid-derived suppressor cells. Nat.Rev.Cancer. 2013; 13:739–752. [PubMed: 24060865]

Vasquez-Dunddel D, Pan F, Zeng Q, Gorbounov M, Albesiano E, Fu J, Blosser RL, Tam AJ, Bruno T, Zhang H, et al. STAT3 regulates arginase-I in myeloid-derived suppressor cells from cancer patients. J.Clin.Invest. 2013

vivar-Valderas A, Salas E, Bobrovnikova-Marjon E, Diehl JA, Nagi C, Debnath J, guirre-Ghiso JA. PERK integrates autophagy and oxidative stress responses to promote survival during extracellular matrix detachment. Mol.Cell Biol. 2011; 31:3616–3629. [PubMed: 21709020]

Ye J, Kumanova M, Hart LS, Sloane K, Zhang H, De Panis DN, Bobrovnikova-Marjon E, Diehl JA, Ron D, Koumenis C. The GCN2-ATF4 pathway is critical for tumour cell survival and proliferation in response to nutrient deprivation. EMBO J. 2010; 29:2082–2096. [PubMed: 20473272]

zwaan-McCabe D, Riordan JD, Arensdorf AM, Icardi MS, Dupuy AJ, Rutkowski DT. The Stress-Regulated Transcription Factor CHOP Promotes Hepatic Inflammatory Gene Expression, Fibrosis, and Oncogenesis. PLoS.Genet. 2013; 9:e1003937. [PubMed: 24367269]

NIH-PA Author Manuscript

NIH-PA Author Manuscript

NIH-PA Author Manuscript

NIH-PA Author Manuscript
NIH-PA Author Manuscript
NIH-PA Author Manuscript

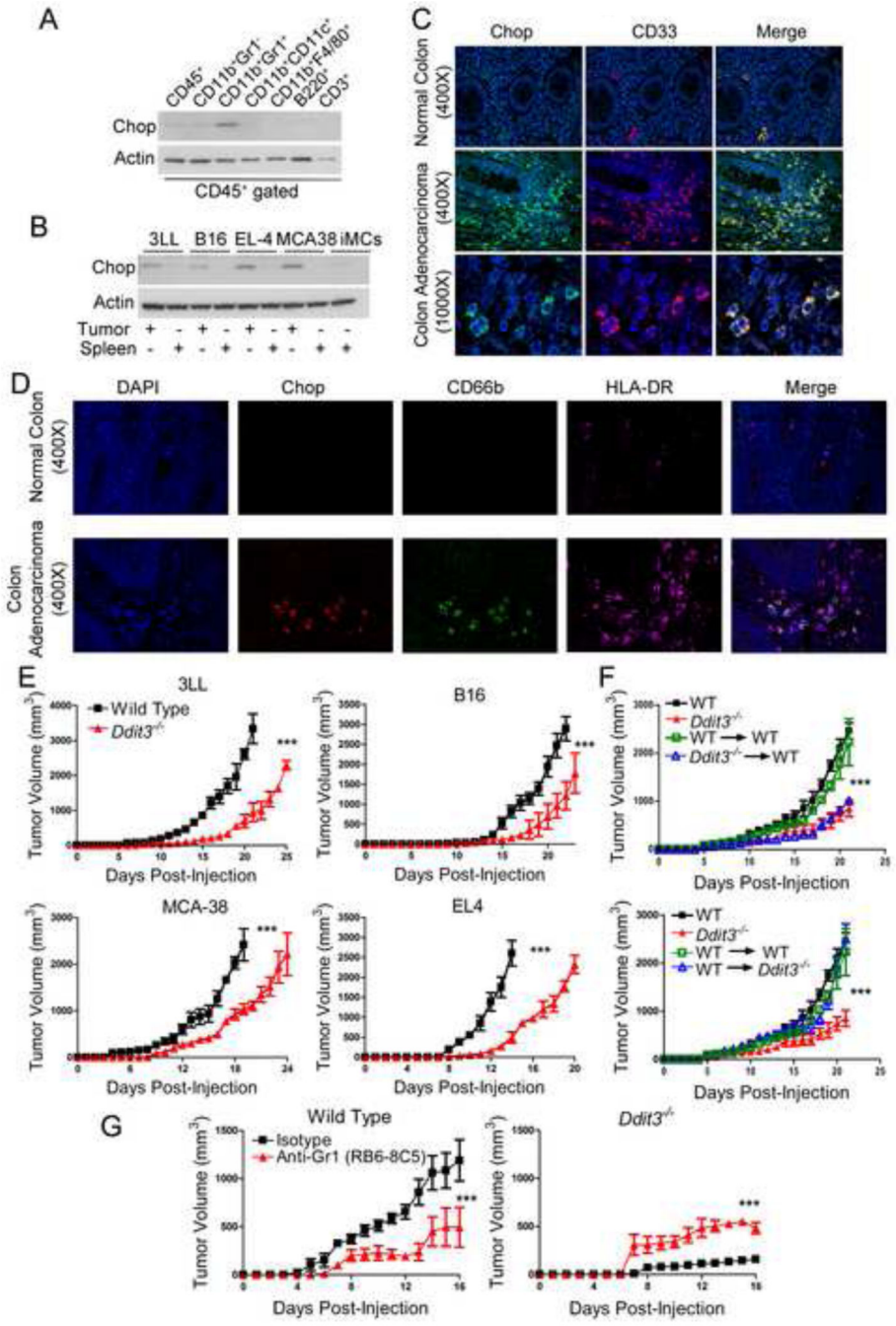

Figure 1. Stromal Chop deletion delays tumor progression in a MDSCs-dependent manner

(A) Chop levels in specific stromal cell populations sorted by flow cytometry from single cell suspensions of s.c. 3LL tumors 18 days after injection.

(B) Chop expression in splenic and tumor-MDSCs recovered from mice bearing s.c. 3LL lung carcinoma, B16 melanoma, EL-4 thymoma, or MCA-38 colon carcinoma. Immature myeloid cells (iMCs) were obtained by sorting $CD11b^{+}$ $Gr1^{+}$ cells from spleens of mice without tumors.

NIH-PA Author Manuscript

NIH-PA Author Manuscript

NIH-PA Author Manuscript

(C) Immunofluorescence detection of Chop (Alexa Fluor 488 secondary antibody - green) and $CD33^+$ (Alexa Fluor 590 secondary antibody - red) in a panel of biopsies from advanced colon carcinoma patients. A representative slide from 24 patients.
(D) Immunofluorescence detection of Chop (Alexa Fluor 590 - red), CD66b (Alexa Fluor 488 - green) and HLA-DR (Alexa Fluor 647 - pink) in tissues from C.
(E) Tumor growth kinetics in wild type (WT – closed square) and *Ddit3*$^{-/-}$ mice (closed triangle) bearing s.c. 3LL lung carcinoma, B16 melanoma, EL-4 thymoma, or MCA-38 colon carcinoma. Average kinetics ± SEM of 10 mice per group from two replicates.
(F) Lethally irradiated wild type $CD45.1^+$ mice received bone marrow transplants from $CD45.2^+$ wild type (WT→WT, green open square) or $CD45.2^+$ *Ddit3*$^{-/-}$ (*Ddit3*$^{-/-}$ →WT, blue open triangle). Seven weeks post-transplant, chimeric mice and non-irradiated wild type $CD45.2^+$ (WT, closed black square) or *Ddit3*$^{-/-}$ $CD45.2^+$ (*Ddit3*$^{-/-}$, closed red triangle) mice were injected s.c. with 3LL cells and tumor growth monitored. For reversal studies, lethally irradiated $CD45.2^+$ wild type (WT→WT, green open square) or $CD45.2^+$ *Ddit3*$^{-/-}$ (WT→ *Ddit3*$^{-/-}$, blue open triangle) were transplanted with $CD45.1^+$ wild type bone marrow and injected s.c. with 3LL cells after seven weeks together with non-irradiated controls. Results expressed as mean ± SEM from 10 mice from two experiments.
(G) 3LL-bearing wild type and *Ddit3*$^{-/-}$ mice were injected either with anti-Gr1 or isotype antibody (i.p. 200 μg/mouse every 4 days) and tumor growth monitored.
In all panels ***$p < 0.001$. See also Figure S1.

NIH-PA Author Manuscript

NIH-PA Author Manuscript

NIH-PA Author Manuscript

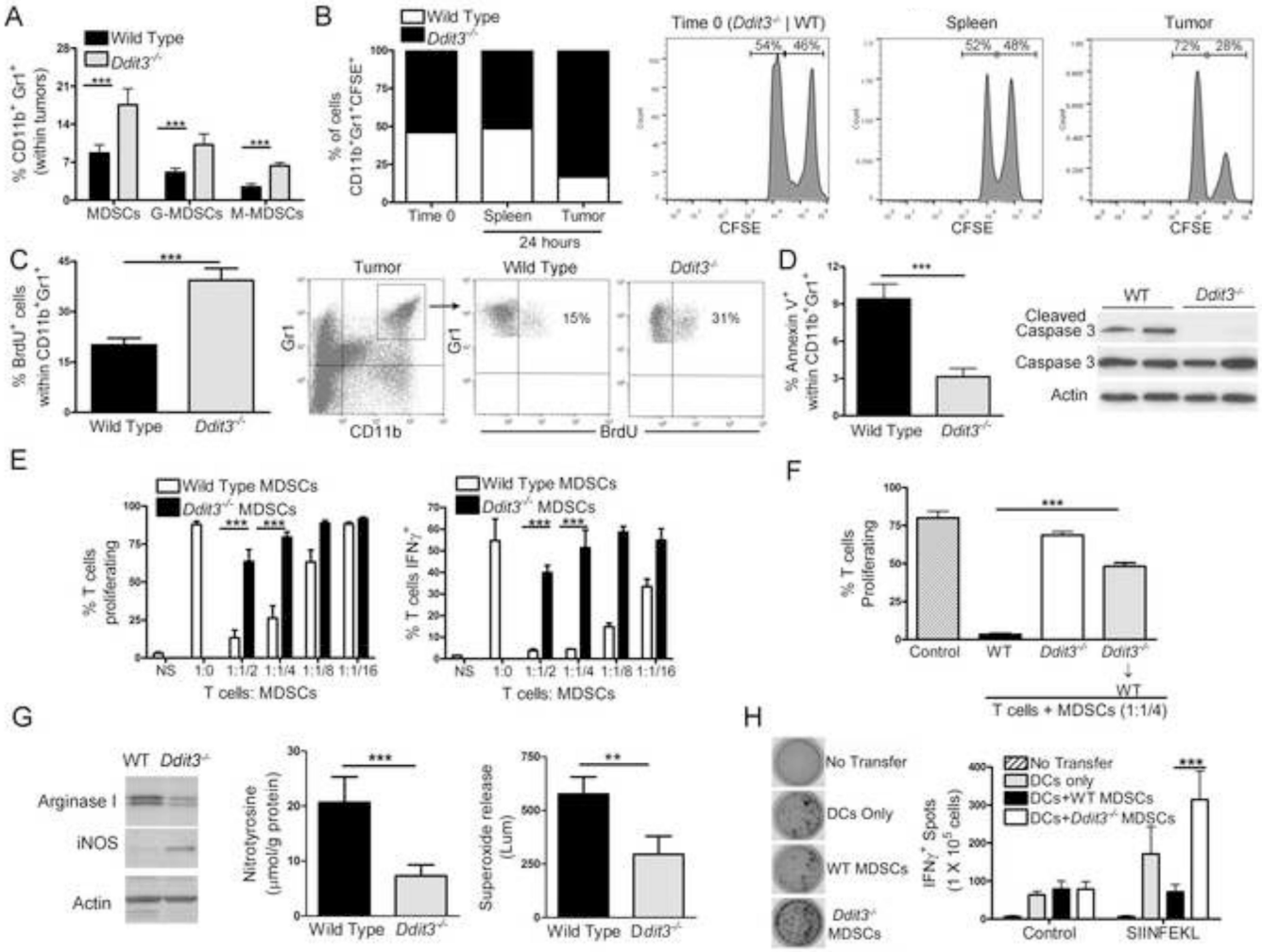

Figure 2. Chop deletion in MDSCs decreases turnover, increases proliferation, and blocks immune tolerogenic function

(A) Percentage of MDSCs ($CD11b^+$ $Gr1^+$), as well as granulocytic (G-MDSCs, $CD11b^+$ $Ly6G^+$ $Ly6C^{Int}$) and monocytic (M-MDSCs, $CD11b^+$ $Ly6G^{lo}$ $Ly6C^{hi}$) subsets in wild type and *Ddit3*$^{-/-}$ mice bearing s.c. 3LL tumors for 17 days.

(B) Bone marrow MDSCs sorted from wild type and *Ddit3*$^{-/-}$ 3LL tumor-bearing mice were labeled with high or low concentration of CFSE, respectively, mixed in a 1:1 ratio, and co-injected i.v. into wild type 3LL bearing mice. Transferred MDSCs accumulation was monitored in the spleen and tumor 24 hours after injection. Representative plot from 2 experiments (n=5).

(C) Wild type and *Ddit3*$^{-/-}$ mice bearing 3LL tumors for 16 days were injected i.p. with BrdU and the percentage of $BrdU^+$ MDSCs (gated within $CD11b^+$ $Gr1^+$) calculated 24 hours later by flow cytometry. Results are mean ± SEM of 5 mice per group in 3 independent experiments.

(D) Percentage of annexin V^+ MDSCs and expression of cleaved and total caspase 3 in tumor-MDSCs from wild type and *Ddit3*$^{-/-}$ mice bearing 3LL tumors for 17 days. Representative plots from 3 experiments (n=10).

NIH-PA Author Manuscript

NIH-PA Author Manuscript

NIH-PA Author Manuscript

(E) CFSE-labeled $CD3^+$ T cells activated with anti-CD3/CD28 were co-cultured at different ratios with MDSCs isolated from wild type and *Ddit3*$^{-/-}$ mice bearing s.c. 3LL tumors for 17 days. Proliferation and IFNγ expression in T cells was monitored 72 hours later. Results are expressed as mean ± SEM from 10 mice per group from 2 experiments.
(F) $CD3^+$ T cells were activated with plated bound anti-CD3/CD28 and co-cultured in a ratio of 1:1/4 with MDSCs sorted from wild type, *Ddit3*$^{-/-}$, or *Ddit3*$^{-/-}$ bone marrow chimeric mice bearing 3LL cells for 17 days. Mean ± SEM from 3 experiments.
(G) Western blot for arginase I and inducible nitric oxide synthase in isolated MDSCs. ELISA for PNT in MDSCs protein lysates. Assay of superoxide production in isolated MDSCs. All assessments performed on MDSCs isolated from wild type or *Ddit3*$^{-/-}$ 3LL tumor-bearing mice 18 days after s.c. injection. Data plotted are pooled values from 3 experiments (n=5).
(H) IFNγ Elispot (representative images in left panel) of SIINFEKL challenged lymph node cells from wild type $CD45.1^+$ mice that received i.v. transfer of $CD45.2^+$ OT-1 cells, SIINFEKL-loaded DCs, and SIINFEKL-pulsed MDSCs from wild type or *Ddit3*$^{-/-}$ mice. Data are expressed as mean ± SEM from 3 experiments having 5 independent samples.
In the figures, $^{**}p < 0.01$, $^{***}p < 0.001$. See also Figure S2.

NIH-PA Author Manuscript
NIH-PA Author Manuscript
NIH-PA Author Manuscript

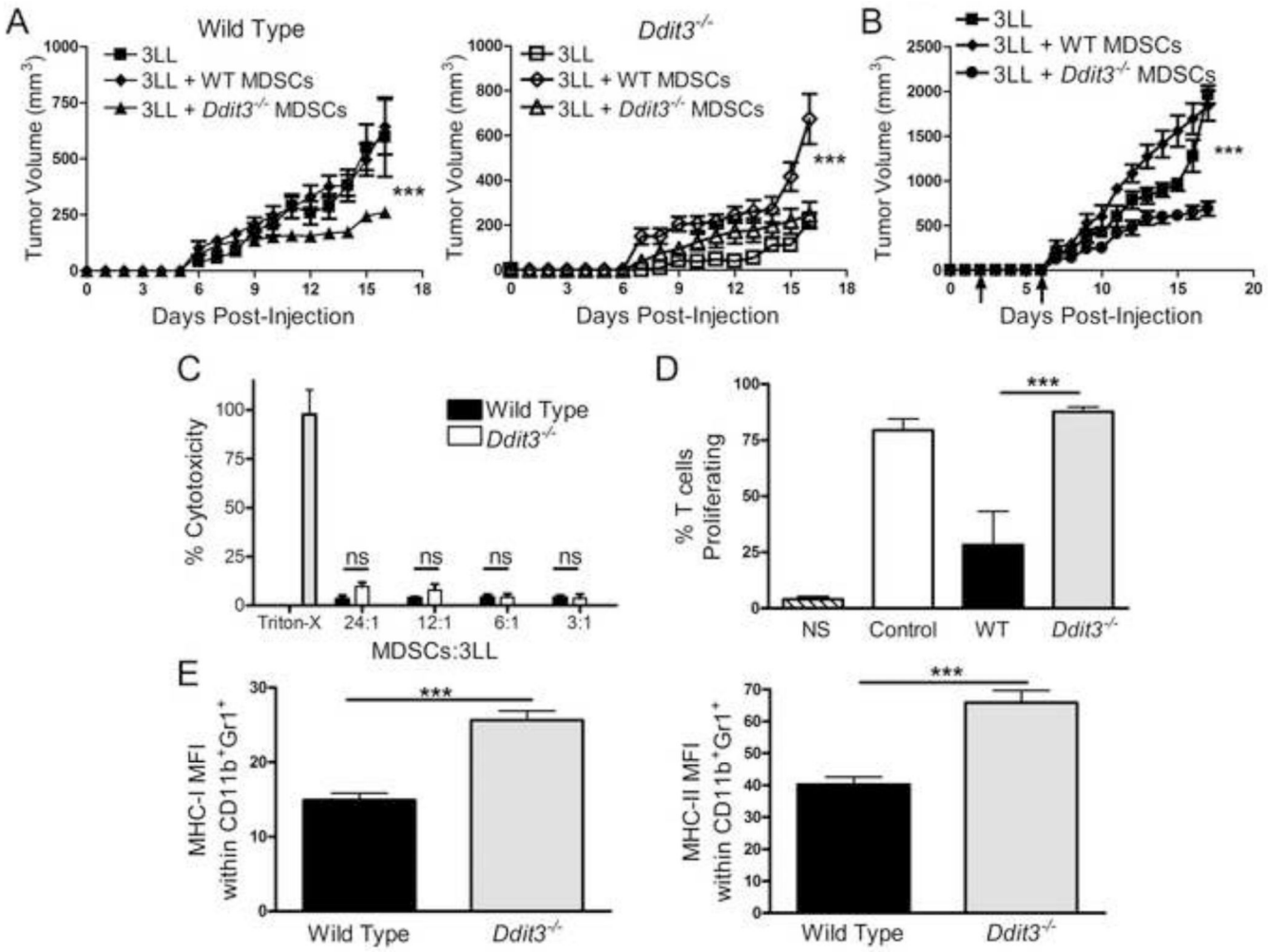

Figure 3. Chop deficient MDSCs delay tumor growth and promote T cell function

(A) Tumor growth in wild type (left panel – closed symbols) and *Ddit3*$^{-/-}$ mice (right panel – open symbols) injected with 3LL cells alone (closed and open squares) or co-injected with tumor-MDSCs from wild type (closed and open diamonds) or *Ddit3*$^{-/-}$ mice (closed and open triangle). Co-injected cells were mixed at a 1:1 ratio. Plots are from 10 mice from 2 experiments.

(B) Tumor growth kinetics in control mice (3LL alone - square) or mice receiving i.v. transfer of wild type (diamond) or *Ddit3*$^{-/-}$ (circle) MDSCs (3×10^6) on days 3 and 6 after 3LL injection.

(C) LDH cytotoxicity assay of 3LL tumor cells after 6 hours of co-culture with MDSCs from wild type or *Ddit3*$^{-/-}$ mice bearing s.c. 3LL tumors for 17 days. Results are from 3 replicates (n=10).

(D) Proliferation of CFSE-labeled CD8$^+$ OT-1 cells after 72 hours of priming with SIINFEKL-pulsed MDSCs from wild type or *Ddit3*$^{-/-}$ mice (2 μg/mL for 4 hours). Results are from 3 replicate experiments.

(E) Mean fluorescent intensity (MFI) of MHC-I and MHC-II in tumor-MDSCs from wild type or *Ddit3*$^{-/-}$ mice. Data are expressed as mean ± SEM from 3 replicates.

In the plots, ***$p < 0.001$.

NIH-PA Author Manuscript
NIH-PA Author Manuscript
NIH-PA Author Manuscript

NIH-PA Author Manuscript
NIH-PA Author Manuscript
NIH-PA Author Manuscript

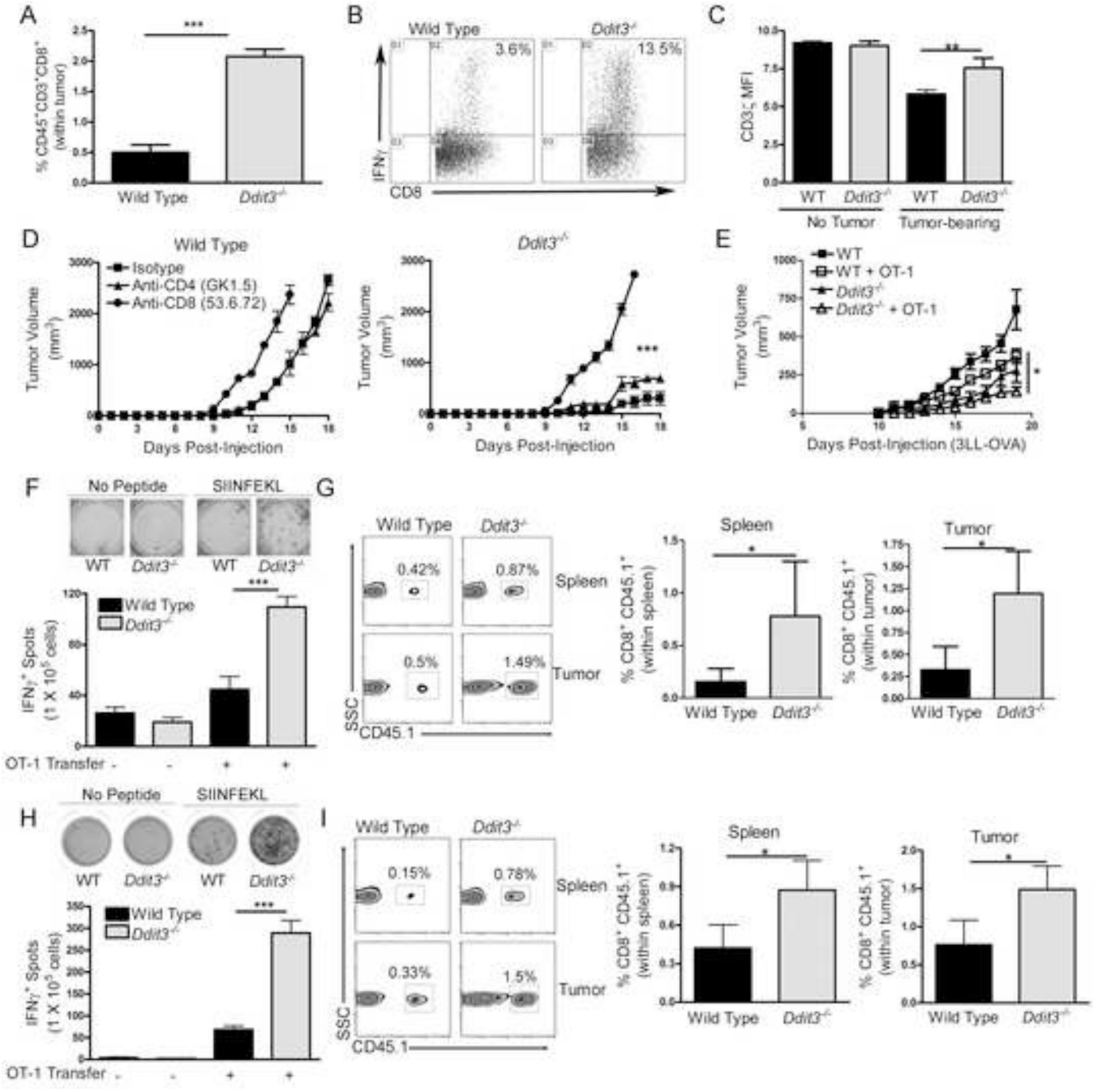

Figure 4. Chop deletion overcomes tumor-induced T cell tolerance and enhances T cell immunotherapy

(A) Percentage of $CD45^+$ $CD3^+$ $CD8^+$ T cells in single cell suspensions of 3LL tumors from wild type and *Ddit3*$^{-/-}$ mice after 17 days of tumor injection.

(B) Percentage of IFNγ-expressing splenic T cells obtained from wild type or *Ddit3*$^{-/-}$ tumor-bearing mice and activated *in vitro* with anti-CD3/CD28 for 48 hours.

(C) Mean fluorescent intensity (MFI) of CD3ζ in splenic $CD3^+$ T cells from wild type and *Ddit3*$^{-/-}$ mice bearing or not s.c. 3LL tumors for 17 days.

NIH-PA Author Manuscript

NIH-PA Author Manuscript

NIH-PA Author Manuscript

(D) Tumor growth in 3LL tumor-bearing wild type and *Ddit3*$^{-/-}$ mice treated with antibodies against CD8^{+} or CD4^{+} T cells (isotype – square, anti-CD4 – triangle, anti-CD8 – circle). Data from 5 mice per group.

(E) Wild type and *Ddit3*$^{-/-}$ mice (CD45.2^{+}) bearing s.c. 3LL-OVA tumors for 7 days were left untreated or received adoptive transfer with naïve CD45.1^{+} CD8^{+} OT-1 cells (5×10^{6}), followed by immunization with SIINFEKL. Then, they were followed for tumor growth. Close square – wild type (WT) no adoptive transfer, open square – WT plus OT-1 adoptive transfer, closed triangle – *Ddit3*$^{-/-}$ no adoptive transfer, open triangle – *Ddit3*$^{-/-}$ plus OT-1 adoptive transfer.

(F-G) CD45.2^{+} wild type and *Ddit3*$^{-/-}$ mice bearing 3LL-OVA tumors for 7 days, received 5×10^{6} CD45.1^{+} OT-1 cells, followed by vaccination using SIINFEKL. Representative density plots of IFNγ producing splenocytes ± *in vitro* challenge with 2 μg/mL SIINFEKL (left panel) and percentages (right panels) of CD45.1^{+} CD8^{+} OT-1 cells in the spleen (top) and tumor (bottom) 10 days after the OT-1 cell adoptive transfer.

(H-I) Endpoints as G-H were obtained from wild type and *Ddit3*$^{-/-}$ mice bearing equal sized tumors of 3LL-OVA. Elispot results from 10 mice per group from 3 independent experiments.

In the figures, *p <0.05, **p<0.01, ***p<0.001. See also Figure S3.

NIH-PA Author Manuscript
NIH-PA Author Manuscript
NIH-PA Author Manuscript

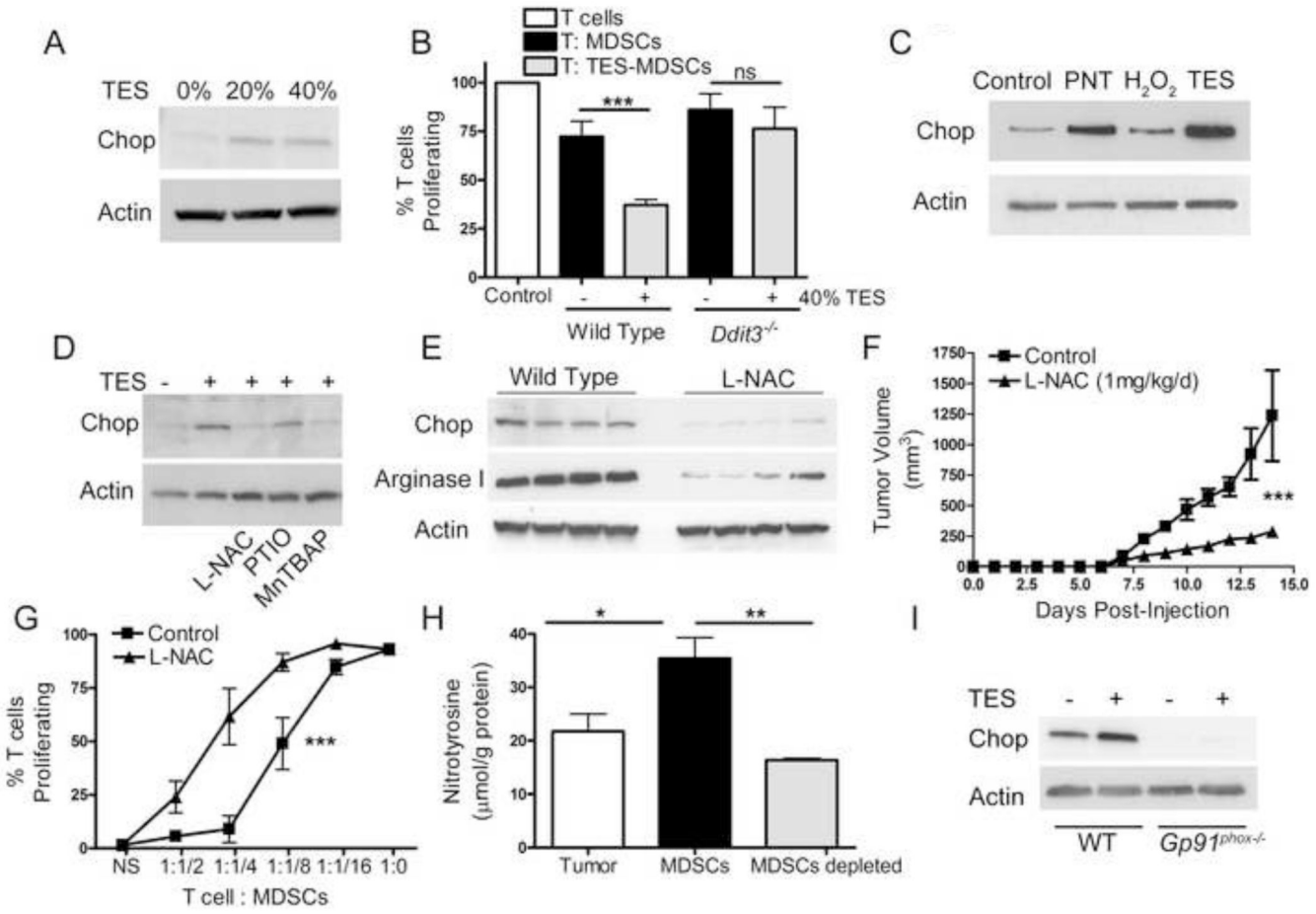

Figure 5. Tumor-derived stress factors trigger Chop expression in MDSCs

(A) Chop expression in BM-MDSCs generated after culture of bone marrow precursors with G-CSF (100 ng/mL) and GM-CSF (20 ng/mL) and treated with tumor explants supernatants (TES) during the last 24 hours. TES was obtained from cell-free supernatants of wild type 3LL tumor digests incubated overnight at 1×10^7 cells/mL.

(B) Co-culture of CFSE-labeled T cells with TES-primed wild type and *Ddit3*$^{-/-}$ BM-MDSCs at a 1:1/4 ratio for 72 hours. Proliferation calculated by CFSE and normalized to activated T cells without BM-MDSCs co-culture.

(C) Chop expression in BM-MDSCs exposed during the last 24 hours of culture to PNT (250 µM) or hydrogen peroxide (250 µM).

(D) Chop expression in BM-MDSCs ± 40% TES with or without the addition of 2 mM L-NAC, 100 µM PTIO, or 100 µM MnTBAP.

(E) Chop and arginase I expression in MDSCs from 3LL-bearing mice treated daily i.p. with PBS or 1 mg/kg L-NAC.

(F) Tumor progression in mice with PBS or 1 mg/kg L-NAC. N=10 from 2 experiments.

(G) Proliferation of CFSE-labeled T cells 72 hours after co-culture with different numbers of tumor-MDSCs recovered from PBS or L-NAC treated-3LL tumor-bearing mice.

(H) ELISA for nitrotyrosine in extracts prepared from single cell 3LL tumor digests as well as MDSCs sorted and MDSCs-depleted fractions.

(I) Expression of Chop in TES-treated wild type and *Gp91*$^{phox-/-}$ BM-MDSCs.

In all panels, data are expressed as mean ± SEM from a representative experiment of 3 replicates. ***$p < 0.001$. See also Figure S4.

NIH-PA Author Manuscript
NIH-PA Author Manuscript
NIH-PA Author Manuscript

NIH-PA Author Manuscript
NIH-PA Author Manuscript
NIH-PA Author Manuscript

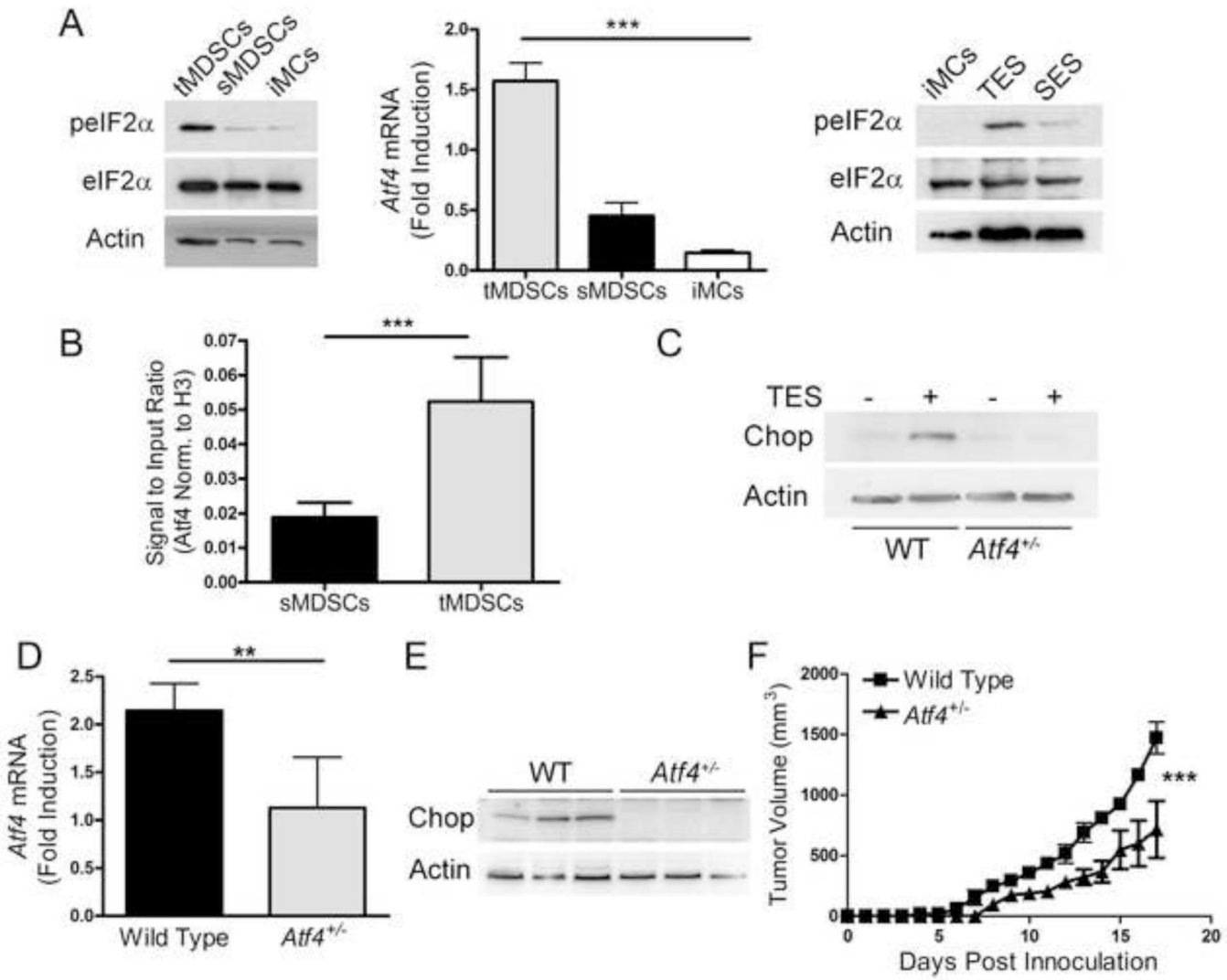

Figure 6. Atf4 regulates tumor-induced Chop expression in MDSCs

(A) Phosphorylation of eIF2α (left panel) and mRNA expression of Atf4 (center panel) in tumor and spleen-MDSCs from 3LL-bearing mice or iMCs from controls. eIF2α phosphorylation in iMCs cultured for 24 hours in the presence of TES or spleen explants supernatant (SES) (right panel). Atf4 mRNA expression in tumor-MDSCs (tMDSCs) or spleen-MDSCs (sMDSCs) or immature myeloid cells (iMCs) sorted from naïve spleens.

(B) ChIP assay of MDSCs-chromatin immunoprecipitated using anti-Atf4 antibodies and assayed for Chop promoter by RT-PCR. Data from n=5 mice per group.

(C) Expression of Chop in TES-treated wild type and *Atf4*$^{+/-}$ BM-MDSCs.

(D-E) Atf4 mRNA and Chop expression in tumor-MDSCs from wild type and *Atf4*$^{+/-}$ bearing s.c. 3LL tumors. Data from 5 mice per group.

(F) Tumor growth in wild type (WT – closed square) and *Atf4*$^{+/-}$ mice (closed triangle) bearing 3LL tumors. Average kinetics ± SEM of 10 mice per group from two replicates.

In the figures, **p<0.01, ***p<0.001.

NIH-PA Author Manuscript
NIH-PA Author Manuscript
NIH-PA Author Manuscript

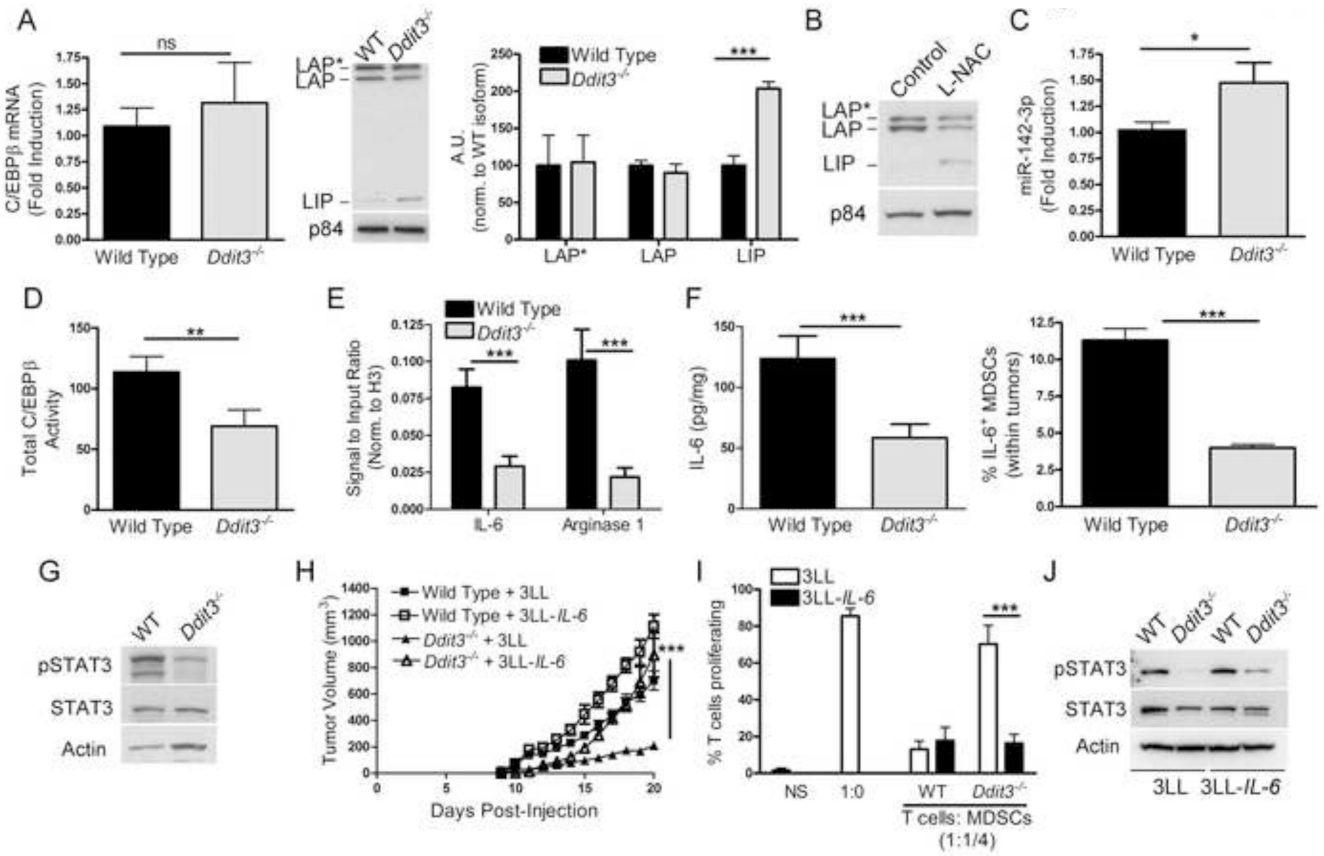

Figure 7. Deletion of Chop blocks tumor growth and MDSCs function through inhibition of IL-6 production

(A) Expression of C/EBPβ mRNA in tumor-MDSCs sorted from wild type and *Ddit3*$^{-/-}$ mice bearing 3LL tumors (left panel). C/EBPβ isoform LAP, LAP*, and LIP expression in nuclear lysates from wild type and *Ddit3*$^{-/-}$ MDSCs at tumor endpoint (right panel). Densitometric analysis of isoforms from 3 experiments.

(B) Expression of LAP, LAP*, and LIP in nuclear lysates from tumor-MDSCs isolated from PBS and L-NAC-treated 3LL tumor-bearing wild type mice.

(C) Expression of mature miR-142-3p in tumor-MDSCs from wild type and *Ddit3*$^{-/-}$ 3LL tumor-bearing mice.

(D) DNA-binding ELISA for C/EBPβ in MDSCs nuclear lysates. Data from 5 independent samples per group.

(E) MDSCs-Chromatin obtained from wild type and *Ddit3*$^{-/-}$ mice bearing s.c. 3LL tumors for 17 days was immunoprecipitated with anti-C/EBPβ antibodies and analyzed by RT-PCR for C/EBPβ-binding sequences on IL-6 and Arginase I promoters. Data from n=5 samples per group.

(F) IL-6 levels in whole cell extracts from wild type and *Ddit3*$^{-/-}$ tumor-MDSCs (left panel). Percentage of IL-6^{+} MDSCs in tumor digests 5 hours after i.p. injection of Brefeldin A (right panel). Data from n=5 samples per group.

(G) STAT3 phosphorylation in wild type and *Ddit3*$^{-/-}$ tumor-MDSCs.

NIH-PA Author Manuscript

NIH-PA Author Manuscript

NIH-PA Author Manuscript

(H) Tumor growth in wild type or *Ddit3*$^{-/-}$ mice injected with mock or IL-6 over expressing 3LL cells (3LL mock – wild type (closed square) and *Ddit3*$^{-/-}$ (closed triangle) (3LL-*IL-6* – wild type (open square) and *Ddit3*$^{-/-}$ (open triangle)).

(I) T cell proliferation after co-culture with tumor-MDSCs from wild type and *Ddit3*$^{-/-}$ mice bearing s.c. mock or IL-6 over expressing 3LL cells. T cell proliferation plotted at a co-culture dilution of 1:1/4 T cells: MDSCs.

(J) STAT3 phosphorylation in MDSCs from wild type or *Ddit3*$^{-/-}$ mice injected with mock or IL-6 over expressing 3LL tumors.

Data was expressed as mean ± SE from a representative experiment of 3 experiments unless otherwise stated. Ns: non-significant, *p <0.05, **p<0.01, ***p<0.001. See also Figure S5.